Article ID: 1000-324X(2022)12-1351-07 **DOI:** 10.15541/jim20220179

Crystallization Kinetics, Properties of *α*-cordierite Based Glass-ceramics Prepared by Glass Powder Sintering

SUN Yangshan[1,3], YANG Zhihua[2], CAI Delong[2], ZHANG Zhengyi[1,3], LIU Qi[1,3], FANG Shuqing[1,3], FENG Liang[1,3], SHI Lifen[1,3], WANG Youle[1,3], JIA Dechang[2]

(1. State Key Laboratory of Advanced Technology for Float Glass, CNBM Research Institute for Advanced Glass Materials Group Co., Ltd, Bengbu 233000, China; 2. Key Laboratory of Advanced Structrual-Functional Integration Materials & Green Manufacturing Technology, Harbin Institute of Technology, Harbin 150001, China; 3. Silica-based Materials Laboratory of Anhui Province, Bengbu 233000, China)

Abstract: The resulting glass-ceramics were prepared by glass powder sintering using stoichiometric and non-stoichiometric cordierite components with addition of B_2O_3. Properties of the glass-ceramics, including the non-isothermal crystallization kinetics, thermal, mechanical and dielectric properties were investigated. The *α*-cordierite based glass-ceramics can be easily prepared by using non-stoichiometric cordierite components, and B_2O_3 addition can promote the precipitation of *α*-cordierite and improve the crystallization ability of the MgO-Al_2O_3-SiO_2 glass. Moreover, rich MgO and SiO_2 in the glass composition did not affect the crystallization ability of the glass, but affect the type of precipitated crystal phase. The increase of B_2O_3 addition can prepare *α*-cordierite based glass-ceramics with a low coefficient of thermal expansion (CTE), but it also lower its softening point. In addition, the increase of B_2O_3 addition can also improve the compactness and mechanical strength of the glass-ceramics. The maximum flexural strength, elastic moduli, fracture toughness and bulk density of *α*-cordierite based glass-ceramics are (42.4±3.0) MPa, (34.0±2.9) GPa, (0.7±0.15) MPa·$m^{1/2}$, and 1.53 g/cm^3, respectively. And the as-prepared *α*-cordierite based glass-ceramics show good dielectric properties (*ε* as low as 3.5) with a low CTE of 4.22 × 10^{-6} K^{-1}.

Key words: *α*-cordierite; glass-ceramics; powder sintering; crystallization kinetics; mechanical property; dielectric property

The possible crystal phases in MgO-Al_2O_3-SiO_2 (MAS) based glass-ceramics are mainly cordierite ($2MgO•2Al_2O_3•5SiO_2$), spinel ($MgO•Al_2O_3$), mullite ($3Al_2O_3•2SiO_2$), forsterite ($2MgO•SiO_2$) and quartz (SiO_2) phases, *etc*[1]. Among them, the cordierite phase has received extensive attention due to its excellent mechanical properties, good dielectric properties and low coefficient of thermal expansion (CTE)[2-5]. However, it is difficult to obtain pure cordierite phase glass-ceramics. Most researchers reported that the glass-ceramics with cordierite as the main crystal phase could be obtained by controlling the composition of the raw materials[6-8]. Cordierite based glass-ceramics can be used in many fields, including microelectronics packaging, coatings, low-temperature co-fired ceramic substrates, aerospace, *etc*.[9-13]. The composition range (in mass) of the cordierite based glass-ceramics is 9.5%–25.5% MgO, 17.5%–34.5% Al_2O_3, 49%–68% SiO_2[1], and some nucleating agents, such as TiO_2, ZrO_2, P_2O_5 and CeO_2, *etc.*, are added into the raw materials to promote glass crystallization[6,14-16]. The glass composition (in mass) designed in stoichiometric composition (13.8% MgO, 34.9% Al_2O_3, 51.3% SiO_2) of cordierite has a narrow interval for the formation of the cordierite phase during the heat-treatment. Compared with the stoichiometric composition of cordierite, the composition rich in MgO and SiO_2 can inhibit the formation of *μ*-cordierite and promote the formation of *α*-cordierite in the glass. The Al_2O_3-rich component has no effect on the formation of *α*-cordierite, but enhances the stability of the glass grid structure, so makes crystal precipitation and growth difficult[17]. Adding some sintering aids or nucleating

Received date: 2022-03-30; **Revised date:** 2022-05-25; **Published online:** 2022-06-03
Foundation item: Anhui Provincial Natural Science Foundation (Youth Project) (2008085QE248); Key Research and Development Projects of Anhui Province (202004a05020061, 202004a05020036); The 6th China Association for Science and Technology "Young Talent Support Project"
Biography: SUN Yangshan (1989–), male, senior engineer. E-mail: ashan19890608@163.com
孙扬善(1989–), 男, 高级工程师. E-mail: ashan19890608@163.com

agents will deteriorate the properties of the glass-ceramics, such as larger thermal expansion coefficient and higher dielectric constant[18]. Therefore, in order to prepare cordierite based glass-ceramics with excellent comprehensive properties, the addition of additives must be avoided or reduced.

The preparation methods of MAS system glass ceramics mainly include integral crystallization, powder sintering, Sol-Gel method and solid-state reaction[17]. The integral crystallization method can be used to prepare dense glass-ceramics with controllable crystal-grain size, but it requires the addition of nucleating agents, high temperature and long crystallization time[3,19]. The powder sintering method has the advantages of easy crystallization and unnecessary addition of nucleating agents when preparing glass-ceramics, but it is difficult to prepare dense materials[5]. The advantages of Sol-Gel method are that the preparation temperature is low, the glass composition can be accurately controlled to obtain materials with high purity, but the cost is high and the environment is easily polluted[16]. The solid-phase reaction method has simple preparation process and easy large-scale production, but the reaction temperature and energy consumption are high[20-21]. Choosing which method to prepare α-cordierite based glass-ceramics needs to be decided according to actual experimental conditions and purposes.

Based on the above research on the MAS system of glass-ceramics, two basic components were designed in this work: the stoichiometric component of cordierite, and another component rich in MgO and SiO_2 (nonstoichiometric cordierite). At the same time, the different contents of B_2O_3 were added to the basic ingredients. The addition of B_2O_3 has two functions: reducing the melting temperature of the basic glass component to act as a flux, and promoting the precipitation of α-cordierite in the vitreous[6,22-23]. In this work, α-cordierite based glass-ceramics with excellent comprehensive properties were prepared by glass powder sintering without adding nucleating agents. Moreover, the non-isothermal crystallization kinetics, thermal, mechanical and dielectric properties were investigated.

1 Experimental

1.1 Glass-ceramics preparation

The raw materials was composed of magnesium oxide (purity>98%), alumina (purity>98%), fused quartz (purity>98%) and boron oxide (purity>98%), as shown in Table 1. Two kinds of samples were prepared: (a) sample S, the B_2O_3-added glass-ceramic with stoichiometric cordierite component; (b) samples NS1, NS2 and NS3, the B_2O_3-added glass-ceramics with nonstoichiometric cordierite components (rich in MgO and SiO_2). The raw materials were uniformly mixed by ball milling and passed through a 150 μm (100 mesh) sieve, then melted at 1500 ℃ for 2 h. The high-temperature glass melt was taken out and water-quenched to obtain a loose, transparent glass frits. The glass frits was initially crushed and placed in a silicon nitride tank, using absolute ethanol as the medium. The ball milling process was carried out at a speed of 500 r/min for 2 h. The obtained glass powder was dried, screened through a 74 μm (200 mesh) sieve. The average particle size of the finally glass powder was 5.9 μm. Then, 30 g of glass powder was shaped into a diameter by pressing at 30 MPa in a steel mold. Each component sample was sintered according to the prescribed sintering process, and the resulting glass-ceramics were obtained in a muffle furnace.

1.2 Characterization

The glass powder of each component was tested by differential thermal analysis (DTA; STA449C, Netzsch). And the analysis was performed by heating 50 mg glass powder from room temperature to 1200 ℃ at heating rates of 5, 10, 15 and 20 ℃/min, respectively. The phase compositions of the glass-ceramics were confirmed by X-ray diffraction (XRD, D/max-γB, Ricoh) with CuKα radiation, operating at 40 kV and 100 mA. Scanning electron microscope (SEM, Helios NanoLab 600i, FEI) was used to characterize the morphology of the samples. The CTE of the glass-ceramics was measured by thermal dilatometer (Netzsch, DIL402C). The bulk density and apparent porosity of the glass-ceramics were tested by the Archimedes method using distilled water as the immersion medium liquid[24]. The three-point bending method was used to test the elastic moduli and flexural strength of the glass-ceramics with dimensions of 3 mm × 4 mm × 36 mm. The glass-ceramics was processed into specimens of 2 mm × 4 mm × 20 mm with a notch of 2 mm in depth and 0.2 mm in width for fracture toughness test by the single-edge notched beam (SENB) method. Dielectric constants (ε) and loss tangent (tanδ)

Table 1 Proportion of MAS based glass raw materials (molar percent)

Powder	MgO	Al_2O_3	SiO_2	B_2O_3	Molar ratio of MgO : Al_2O_3 : SiO_2
S	13.80 g (21.38%)	34.90 g (21.19%)	51.30 g (52.8%)	5.00 g (4.45%)	2 : 2 : 5
NS1	24.00 g (33.56%)	22.00 g (12.08%)	54.00 g (50.34%)	5.00 g (4.02%)	6 : 2 : 9
NS2	24.00 g (32.26%)	22.00 g (11.61%)	54.00 g (48.39%)	10.00 g (7.74%)	6 : 2 : 9
NS3	24.00 g (31.06%)	22.00 g (11.18%)	54.00 g (46.58%)	15.00 g (11.18%)	6 : 2 : 9

were measured by RF impedance/material analyzer (PNA N5230A, Agilent) at room temperature.

2 Results and discussion

2.1 DTA and XRD analyses

Fig. 1 presents the DTA curves of the glass powders. The sintering process of each glass-ceramics is formulated based on the DTA curves. That is, the obtained glass-ceramics are prepared by holding at nucleation temperature and crystallization temperature for 1 and 2 h, respectively, at a heating rate of 5 ℃/min.

The phase analysis of each glass-ceramics is shown in Fig. 2. It can be seen that the phase composition of sample S is the mainly *α*-quartz crystal phase, a small amount of spinel and *α*-cordierite phases. This result indicates that the crystallization peak at 999 ℃ on the DTA curve of glass powder S corresponds to *α*-quartz formation, which is firstly precipitated from glass powder S. It is obvious that the phases of samples NS1, NS2 and NS3 are composed of *α*-cordierite as the primary crystalline phase and *α*-quartz and spinel as the

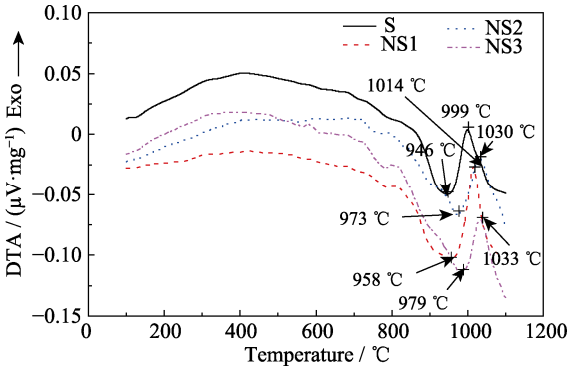

Fig. 1 DTA curves of MAS glass powders at heating rate of 5 ℃/min

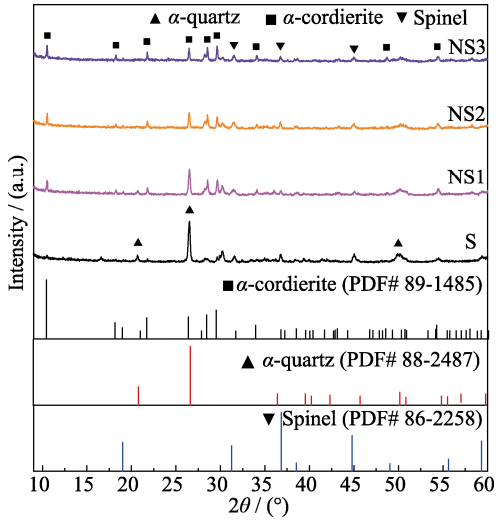

Fig. 2 XRD patterns of the glass-ceramics samples

secondary crystalline phases. Therefore, the crystallization peaks on the DTA curves of glass powder NS1, NS2 and NS3 correspond to *α*-cordierite formation, which is the first crystalline phase to precipitate. According to the results, *α*-cordierite phase is easier to precipitate in the non-cordierite stoichiometric components and increases with the increase of B_2O_3 content in the composition. This result is consistent with the purpose of the initial composition design of the glass-ceramics.

2.2 Non-isothermal crystallization kinetics

Fig. 3 shows the DTA curves of the glass powders at different heating rates. A crystallization peak can be observed on each DTA curve and the crystallization peak temperature (T_p) is obtained. According to the Kissinger equation $\ln(\beta/T_p^2)=\ln(AR/E_k)-E_k/(RT_p)$ (Eq.1)[25], the crystallization activation energy (E_k) of the glass powders can be calculated, where β is the heating rate, R is the molar gas constant (8.314 $J\cdot mol^{-1}\cdot K^{-1}$), and A is the pre-exponential factor. By plotting $\ln(\beta/T_p^2)$ *versus* $1/T_p$, a straight line can be obtained, as shown in Fig. 4. The slope of the line is $-E_k/R$ and the intercept is $\ln(AR/E_k)$, so E_k and A can be calculated. Generally, the value of activation energy E_k is used to judge the crystallization ability of the glass. However, in many heterogeneous reaction systems, the value of E_k is not stable in complex multiphase reactions and cannot be regarded as a constant. Therefore, there are usually some controversies in judging the crystallization ability of a glass system based on the E_k[26-27]. The reaction rate constant $k(T_p)$ at T_P can accurately reflect the crystallization characteristics of the glass, especially in the same glass system, $k(T_p)$ can be used as the judging basis of the crystallization ability of glass. The larger the $k(T_p)$ value, the lower the stability of the glass, the easier it is to crystallize. The $k(T_p)$ value can be calculated according to the Arrhenius equation $k(T_p)= A\cdot\exp(-E_k/RT_p)$ (Eq.2)[25]. The values of A and E_k are calculated from Eq.1. The non-isothermal crystallization kinetic parameters of each group of the glass powders are listed in Table 2.

The $k(T_p)$ values are calculated at heating rates of 5, 10, 15 and 20 ℃/min, respectively, and the average value is given. It can be seen from Table 2 that the $k(T_p)$ value of glass powder NS1 is equivalent to that of glass powder S, indicating that rich MgO and SiO_2 in the MAS glass composition do not affect the crystallization ability of the glass, but affect the type of crystal phase precipitated, as shown in Fig. 2. In the glass powders NS1, NS2 and NS3, it can be found that as the content of B_2O_3 increasing, the value of $k(T_p)$ gradually increases, indicating that B_2O_3 addition can enhance the crystallization ability of the MAS glass. In addition, when the B_2O_3 addition increases from 4.02% to

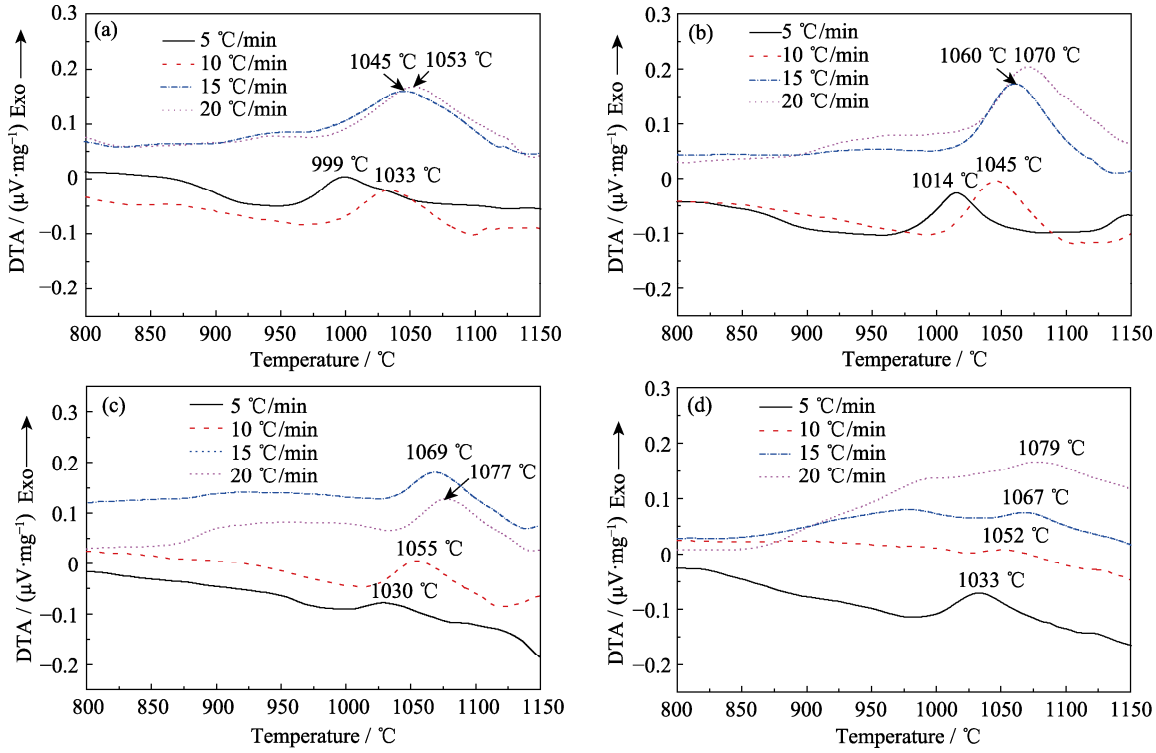

Fig. 3 DTA curves of the glass powders at different heating rates
(a) S; (b) NS1; (c) NS2; (d) NS3

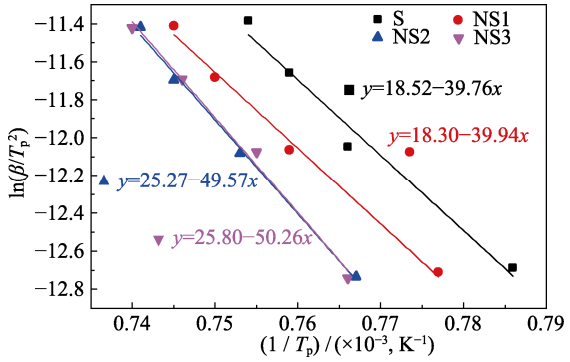

Fig. 4 Plots of $\ln(\beta/T_p^2)$ *versus* $1/T_p$ according to Kissinger equation

Table 2 Non-isothermal crystallization kinetic parameters of the glass powders

Powder	E/(kJ·mol^{-1})	A	k (T_p)				
			5 ℃/min	10 ℃/min	15 ℃/min	20 ℃/min	Mean
S	330.56	4.39×10^{12}	0.117	0.265	0.348	0.417	0.285
NS1	332.06	3.54×10^{12}	0.118	0.245	0.345	0.430	0.285
NS2	412.12	4.68×10^{15}	0.141	0.287	0.424	0.528	0.345
NS3	417.86	8.05×10^{15}	0.156	0.271	0.412	0.580	0.355

7.74%, $k(T_p)$ value increases significantly, while B_2O_3 addition increases from 7.74% to 11.18%, $k(T_p)$ value increases slightly, which indicates that the B_2O_3 addition in the MAS glass beyond 11.18% has little influence on the crystallization ability of the glass.

2.3 Thermal properties

Fig. 5(a) shows the thermal expansion curves of the as-prepared glass-ceramics. The softening point and CTE of the glass-ceramics can be obtained from Fig. 5(a). Compared with other samples, glass-ceramics S has the highest softening point, and no significant deformation occurs below 1300 ℃, which is due to its main crystal phase α-quartz having a higher melting point of about 1750 ℃. The softening points of glass-ceramics NS1, NS2 and NS3 decreased from 1209 ℃ to 941 ℃ successively, indicating that the increase of B_2O_3 content would reduce the softening point of the samples. This is because that B_2O_3 is a low-melting-point oxide, and its addition will lower the softening point of the glass phase, thereby reducing the softening point and service temperature of the glass-ceramics. Therefore, it is not advisable to add excessive B_2O_3 when preparing α-cordierite based glass-ceramics in order to control the service temperature of the resulting glass-ceramics.

Fig. 5(b) shows the CTE of the samples in the temperature range of 100–500 ℃. It can be seen from the figure that the CTE of glass-ceramics S is the largest of about 8.89×10^{-6} K^{-1}. Firstly, it is because that the main crystal phase of glass-ceramics S is α-quartz, which has a large CTE of about 12×10^{-6} K^{-1}[28]. The second reason is that the glass-ceramics S has a higher compactness than other glass-ceramics. The bulk density and apparent porosity of the glass-ceramics are shown in Fig. 6. As the

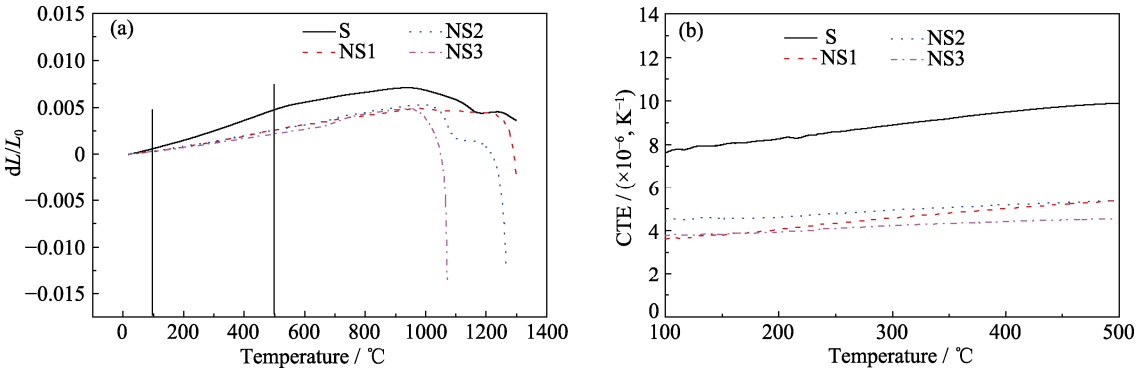

Fig. 5 Thermal expansion curves (a) and CTE (b) of the as-prepared glass-ceramics

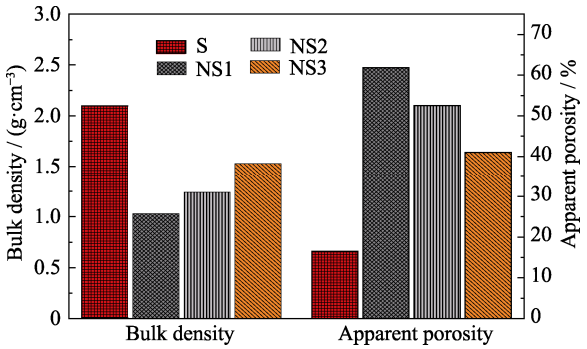

Fig. 6 Bulk density and apparent porosity of the as-prepared glass-ceramics

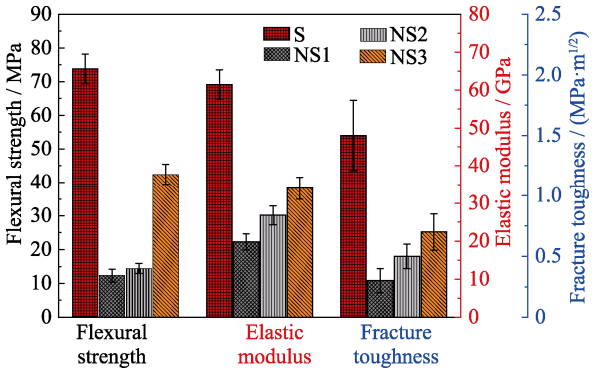

Fig. 7 Mechanical properties of the as-prepared glass-ceramics

CTE of cordierite is about 2.2×10^{-6} K^{-1} and the compactness of glass-ceramics NS1, NS2 and NS3 are relatively low, the CTEs of glass-ceramics NS1, NS2 and NS3 with *α*-cordierite as the main crystal phase are as low as 4.92×10^{-6}, 4.58×10^{-6} and 4.22×10^{-6} K^{-1}, respectively. And with the content of *α*-cordierite increases, the CTEs of the glass-ceramics decrease gradually. It can be found that although the compactness of glass-ceramics NS3 is higher than those of glass-ceramics NS1 and NS2, the CTE of sample NS3 is lower, which is due to the highest content of *α*-cordierite in the glass-ceramics NS3.

2.4 Mechanical properties

Fig. 7 presents the mechanical properties of the as-prepared glass-ceramics. It can be seen that the changing trends of flexural strength, elastic moduli and fracture toughness of different samples are consistent. Since the glass-ceramics prepared in present work have a high apparent porosity, their mechanical properties are mainly related to the porosity rather than the phase composition, that is, the smaller the porosity is, the better the mechanical properties are. Therefore, glass-ceramics S has better mechanical properties due to its high compactness. And the mechanical properties of glass-ceramics NS1, NS2 and NS3 are sequentially enhanced due to the compactness improvement. The *α*-cordierite based glass-ceramics NS3 have the largest flexural strength, elastic moduli and fracture toughness of (42.4±3.0) MPa, (34.0±2.9) GPa and (0.7±0.15) MPa·m$^{1/2}$, respectively.

The microstructure difference of each sample can be clearly seen from Fig. 8. Although the microstructure of glass-ceramics S also contains many pores with diameters of only a few microns, compared with other samples, glass-ceramics S is the densest with a bulk density of 2.10 g/cm^3 and an apparent porosity of 16.5%. Fig. 8(b-d) show that the amount of pores decreases with the content increase of B_2O_3 in the *α*-cordierite based glass-ceramics. The bulk density of glass-ceramics NS1, NS2 and NS3 increased from 1.03 g/cm^3 to 1.53 g/cm^3,

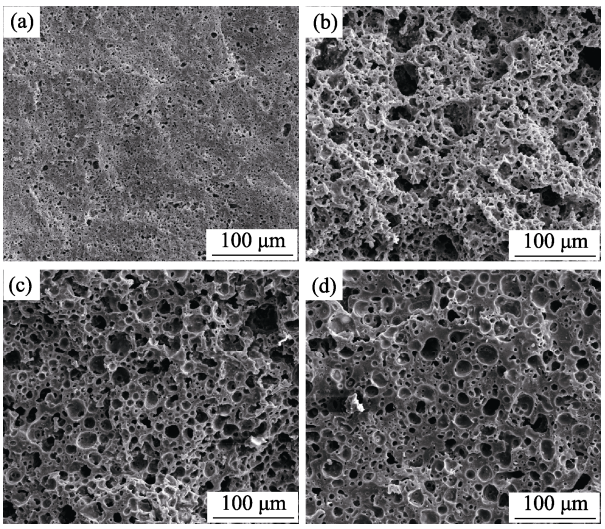

Fig. 8 Morphologies of the as-prepared glass-ceramics
(a) S; (b) NS1; (c) NS2; (d) NS3

and the apparent porosity decreased from 61.8% to 40.9%. The above results indicate that B_2O_3 can promote the density and strength of the sintered glass-ceramics due to the formation of more low-viscosity glass phases during the sintering.

2.5 Dielectric properties

Fig. 9 shows the ε and tanδ of the as-prepared glass-ceramics. Generally, the dielectric properties of porous materials are mainly affected by porosity and phase composition[29]. However, in this work, the ε and tanδ of the as-prepared α-cordierite based glass-ceramics are mainly affected by the porosity, because the porosity of the glass-ceramics is high, and the ε and tanδ of the pores are regarded as 1 and 0, respectively. The ε of α-cordierite glass-ceramics is reported in the range of 5.0–5.5[30]. As shown in Fig. 9(a), the ε values of as-prepared α-cordierite based glass-ceramics are all lower than 3.5 due to the existence of a large number of pores. And the tanδ values of α-cordierite based glass-ceramics are all lower than 4.5×10^{-3} as shown in Fig. 9(b). In addition, among the α-cordierite based glass-ceramics samples, the ε and tanδ values of glass-ceramics NS3 are higher than those of glass-ceramics NS1 and NS2, which is because that glass-ceramics NS3 is denser than glass-ceramics NS1 and NS2. The above results indicate that when the other properties of α-cordierite based glass-ceramics are satisfied, proper introduction of some pores is helpful to reduce the ε and tanδ, and improve the dielectric properties of the glass-ceramics.

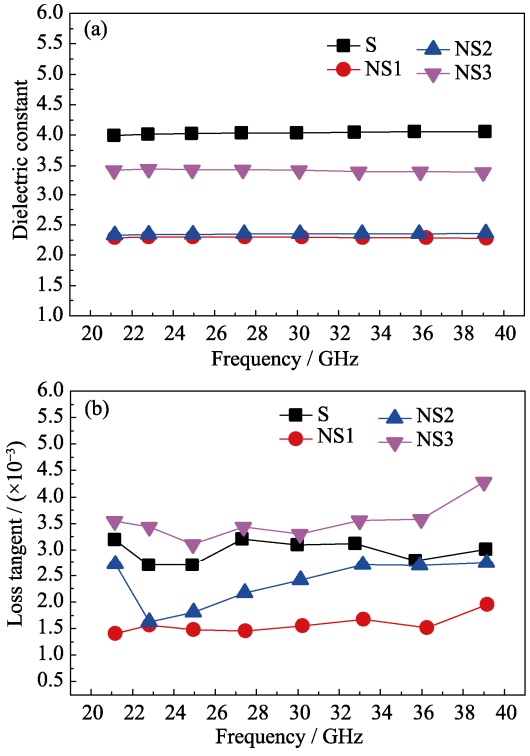

Fig. 9 Dielectric constant (a) and loss tangent (b) of the as-prepared glass-ceramics

3 Conclusions

α-cordierite based glass-ceramics were synthesized by glass powder sintering using MAS glass with the addition of B_2O_3. The effects of composition on the phases, non-isothermal crystallization kinetics, thermal, mechanical and dielectric properties were investigated in detail. MgO and SiO_2 rich in the glass composition and the increase in B_2O_3 content contributed to the precipitation of α-cordierite. Additionally, the increase of B_2O_3 content improved the crystallization ability of the MAS glass and the compactness of the glass-ceramics, and lowered the CTE and softening point of the glass-ceramics. The α-cordierite based glass-ceramics with an apparent porosity of 40.9% had a low CTE of 4.22×10^{-6} K^{-1}, and its flexural strength, elastic moduli, fracture toughness and bulk density were (42.4±3.0) MPa, (34.0±2.9) GPa, (0.7±0.15) MPa·$m^{1/2}$ and 1.53 g/cm^3, respectively. Moreover, the as-prepared α-cordierite based glass-ceramics exhibited good dielectric properties (ε<3.5, tanδ<4.5×10^{-3}). The results show that α-cordierite based glass- ceramics prepared by glass powder sintering is a promising candidate material for structure/function integration.

References:

[1] ZHI M S. Sintering additives to eliminate interphases in cordierite ceramics. *Journal of the American Ceramic Society*, 2010, **88(5):** 1297–1301.

[2] OKUYAMA M, FUKUI T, SAKURAI C. Phase transformation and mechanical properties of B_2O_3-doped cordierite derived from complex-alkoxide. *Journal of Materials Science*, 1993, **28(16):** 4465–4470.

[3] HUA S, LIANG K, FENG Z, *et al*. Characterization of cordierite-based glass-ceramics produced from fly ash. *Journal of Non-Crystalline Solids*, 2004, **337(2):** 157–160.

[4] SUNG Y M. Mechanical properties of α-cordierite and β-spodumene glass-ceramics prepared by sintering and crystallization heat treatments. *Ceramics International*, 1997, **23(5):** 401–407.

[5] YU Y, HAO X, SONG L, *et al*. Synthesis and characterization of single phase and low temperature co-fired cordierite glass-ceramics from perlite. *Journal of Non-Crystalline Solids*, 2016, **448:** 36–42.

[6] RAO R T. Ceramic and glass-ceramic packaging in the 1990s. *Journal of the American Ceramic Society*, 1991, **74(5):**895–908.

[7] WANG S, LIANG K. Crystallization behavior and infrared radiation property of nickel-magnesium cordierite based glass-ceramics. *Journal of Non-Crystalline Solids*, 2008, **354(14):** 1522–1525.

[8] SUN Y, CAI D, YANG Z, *et al*. Effect of holding time on microstructure, mechanical, water resistance and dielectric properties of α-cordierite glass-ceramic coating on porous BN/Si_2N_2O ceramic. *Ceramics International*, 2018, **44(13):** 15764–15769.

[9] WANG F, ZHANG W, CHEN X, *et al*. Synthesis and characterization of low CTE value La_2O_3-B_2O_3-CaO-P_2O_5 glass/cordierite composites for LTCC application. *Ceramics International*, 2019, **45(6):**

7203–7209.
[10] PRUNIER A R. Strengthened cordierite having minor amounts of calcia. US Patent 4745092, 1988.05.17.
[11] WU J M, SHIANG H W. Effect of (B_2O_3, P_2O_5) additives on microstructural development and phase-transformation kinetics of stoichiometric cordierite glass. *Journal of the American Ceramic Society*, 2010, **83(5):** 1259–1265.
[12] BANJURAIZAH J, MOHAMAD H, AHMAD ZA. Densification and crystallization of nonstoichiometric cordierite glass with excess MgO synthesized from kaolin and talc. *Journal of the American Ceramic Society*, 2011, **94(3):** 687–694.
[13] BANJURALIZA J, MOHARMAD H, AHMAD Z A. Synthesis and characterization of xMgO-1.5Al_2O_3-5SiO_2 (x=2.6–3.0) system using mainly talc and kaolin through the glass route. *Materials Chemistry and Physics*, 2011, **129(3):** 910–918.
[14] GOEL A, SHAABAN E R, MELO F, *et al.* Non-isothermal crystallization kinetic studies on MgO-Al_2O_3-SiO_2-TiO_2 glass. *Journal of Non-Crystalline Solids*, 2007, **353(24/25):** 2383–2391.
[15] HAN L, SONG J, LIN C, *et al*. Crystallization, structure and properties of MgO-Al_2O_3-SiO_2 highly crystalline transparent glass-ceramics nucleated by multiple nucleating agents. *Journal of the European Ceramic Society*, 2018, **38(13):** 4533–4542.
[16] SHI Z, LIANG K, ZHANG Q, *et al*. Effect of cerium addition on phase transformation and microstructure of cordierite ceramics prepared by Sol-Gel method. *Journal of Materials Science*, 2001, **36(21):** 5227–5230.
[17] MCMILAN P W. Glass-Ceramics, London: Academic press, 1964.
[18] MEI S, YANG J, FERREIRA J. The densification and morphology of cordierite-based glass-ceramics. *Materials Letters*, 2001, **47(4/5):** 205–211.
[19] CHAO C H, LU H Y. Crystallization of Na_2O-doped colloidal gel-derived silica. *Materials Science and Engineering: A*, 2000, **282(1/2):** 123–130.
[20] MALACHEVSKY M T, FISCINA J E, ESPARZA D A. Preparation of synthetic cordierite by solid-state reaction *via* bismuth oxide flux. *Journal of the American Ceramic Society*, 2001, **84(7):** 1575–1577.
[21] DYATLOVA E M, MINENKOVA G Y, KOLONTAEVA T V. Intensification of sintering of mullite-cordierite ceramics using mineralizers. *Glass and Ceramics*, 2000, **57(11/12):** 427–430.
[22] REBEN M, HONG L. Thermal stability and crystallization kinetics of MgO-Al_2O_3-B_2O_3-SiO_2 glasses. *International Journal of Applied Glass Science*, 2011, **2(2):** 96–107.
[23] LUO W, BAO Z, JIANG W, *et al*. Effect of B_2O_3 on the crystallization, structure and properties of MgO-Al_2O_3-SiO_2 glass-ceramics. *Ceramics International*, 2019, **45(18):** 24750-24756.
[24] WANG X, RUAN J M, CHEN Q Y. Effects of surfactants on the microstructure of porous ceramic scaffolds fabricated by foaming for bone tissue engineering. *Materials Research Bulletin*, 2009, **44(6):** 1275–1279.
[25] KISSINGER H E. Reaction kinetics in differential thermal analysis. *Analytical Chemistry*, 1957, **29(11):** 1702–1706.
[26] FOKIN V M, YURITSYN N S, ZANOTTO E D. Nucleation and crystallization kinetics in silicate glasses: theory and experiment. in nucleation theory and applications. Wiley-VCH Verlag GmbH & Co. KGaA, 2005.
[27] FLYNN J H. Thermal analysis kinetics—past, present and future. *Thermochimica Acta*, 1992, **203:** 519–526.
[28] HÖLLAND W, BEALL G. Glass-ceramic technology. Westernville: The American Ceramic Society, 2002.
[29] WANG S, JIA D, YANG Z, *et al*. Effect of BN content on microstructures, mechanical and dielectric properties of porous BN/Si_3N_4 composite ceramics prepared by gel casting. *Ceramics International*, 2013, **39(4):** 4231–4237.
[30] BANJURAIZAH J, MOHAMAD H, AHMAD Z A. Crystal structure of single phase and low sintering temperature of *α*-cordierite synthesized from talc and kaolin. *Journal of Alloys and Compounds*, 2009, **482(1/2):** 429–436.

粉末烧结法制备 *α*-堇青石基玻璃陶瓷的析晶动力学和性能

孙扬善[1,3], 杨治华[2], 蔡德龙[2], 张正义[1,3], 柳 琪[1,3],
房树清[1,3], 冯 良[1,3], 石丽芬[1,3], 王友乐[1,3], 贾德昌[2]

(1. 中建材玻璃新材料研究院集团有限公司, 浮法玻璃新技术国家重点实验室,, 蚌埠 233000; 2. 哈尔滨工业大学, 结构功能一体化材料及其绿色制造技术工信部重点实验室, 哈尔滨 150001; 3. 安徽省硅基材料实验室, 蚌埠 233000)

摘 要: 在堇青石化学计量组分和非堇青石化学计量组分中分别添加 B_2O_3, 通过玻璃粉末烧结法制备玻璃陶瓷,并研究了玻璃陶瓷的性能, 包括非等温析晶动力学、热学、力学和介电性能。本研究使用非堇青石化学计量组分制备了 α-堇青石基玻璃陶瓷, 并加入 B_2O_3 促进 *α*-堇青石析出, 提高 MgO-Al_2O_3-SiO_2 玻璃的结晶能力。玻璃成分中过量的 MgO 和 SiO_2 不会影响玻璃的析晶能力, 但会影响析晶的类型; 增加 B_2O_3 含量可以制备低热膨胀系数的 *α*-堇青石基玻璃陶瓷, 但会降低玻璃陶瓷的软化点。此外, 增加 B_2O_3 含量还可以提高玻璃陶瓷的致密性和强度。*α*-堇青石基玻璃陶瓷的最大抗弯强度、弹性模量、断裂韧性和体积密度分别为(42.4±3.0) MPa、(34.0±2.9) GPa、(0.7±0.15) MPa·$m^{1/2}$ 和 1.53 g/cm^3。制备的 *α*-堇青石基玻璃陶瓷表现出良好的介电性能(介电常数低至 3.5), 热膨胀系数低至 4.22×10^{-6} K^{-1}。

关 键 词: *α*-堇青石; 玻璃陶瓷; 粉末烧结; 析晶动力学; 力学性能; 介电性能

中图分类号: TQ174 **文献标志码:** A